Available online at www.sciencedirect.com
ScienceDirect
Computers and Mathematics with Applications 53 (2007) 1615–1626
An International Journal
computers & mathematics
with applications
www.elsevier.com/locate/camwa

Numerical models for 2D free boundary analysis of groundwater in slopes stabilized by drain trenches

B. D'Acunto[a,*], F. Parente[b], G. Urciuoli[c]

[a] *Università di Napoli Federico II, Dipartimento di Matematica e Applicazioni, via Claudio 21, 80125, Napoli, Italy*
[b] *Bridgestone Technical Centre Europe, via Fosco del Salceto 13, 00129, Roma, Italy*
[c] *Università di Napoli Federico II, Dipartimento di Ingegneria Geotecnica, via Claudio 21, 80125, Napoli, Italy*

Received 31 May 2006; accepted 2 June 2006

Abstract

A numerical model for 2D free boundary analysis of groundwater in slopes stabilized by drain trenches has been developed. It consists of a front-tracking method (based on an original way of adapting the space derivatives), very effective in saving calculation time respect to classical fix-grid methods. The method analyses the trenches effect inside slopes in which the soils above the water table are partially saturated, for which a boundary can be recognized between the saturated domain (water table) and the unsaturated one (above the water table). In this case pore pressure lowering, due to trenches, can be analyzed considering the progressively reduction of the saturated domain. This approach efficiently solves the problem of fixing hydraulic boundary conditions on the sides of the trenches. Results have been compared with those obtained by a fix-grid method, observing difference less than 0.14%. Applying the method, the capability of drain trenches to control the effect of heavy rainfalls has been investigated, calculating (during the transient process of water table lowering) limit values of water recharge for which water table keeps on constant.

Keywords: Numerical models; Drain trenches; Slopes stability; Free boundary problems; Partial differential equations

1. Introduction

Among the control works against landsliding, drain trenches are probably the most widely used in medium and fine grained soils. Drain trenches are excavated and built from the ground surface to a depth well below the water table. The action of drains reduces pore pressures in the subsoil and their seasonal fluctuations; consequently effective stresses and soil shear strength increase. Using drain trenches in slope stabilization is very common, probably because this technology is cheaper than others and very versatile. Drain trenches and drain pipes are undoubtedly the most suitable remedial measures against landslides when the slip surface is deep. When slope analysis is carried out, the increase in the safety factor due to the role of drains must be evaluated taking into account the pore pressure regime along the supposed slip surface, as modified by drains. Therefore, numerical methods should be made available to

* Corresponding author.
E-mail addresses: dacunto@unina.it (B. D'Acunto), francesco.parente@bridgestone-europe.com (F. Parente), gianurci@unina.it (G. Urciuoli).

0898-1221/$ - see front matter © 2007 Elsevier Ltd. All rights reserved.
doi:10.1016/j.camwa.2006.06.013

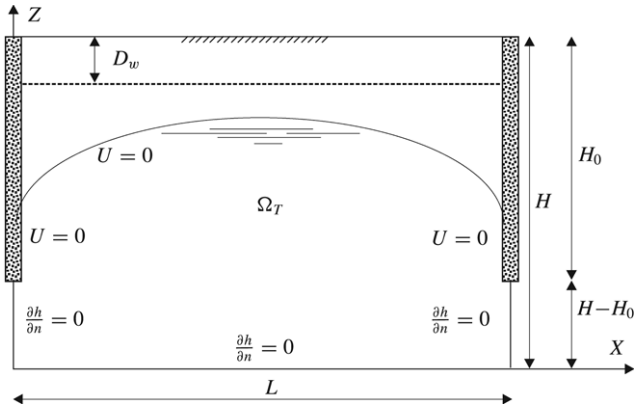

Fig. 1.1. Trench section and boundary conditions.

perform an in-depth analysis of pore pressures in the presence of drains. The case in which the soil above the water table is also saturated, which occurs in fine-grained soils, has already been analysed [1]. Here we consider a typical situation in medium-grained soils, in which soil above the water table is unsaturated. In this situation a boundary can be recognized between the saturated domain (water table) and the unsaturated one (above the water table). The problem can be solved by considering the reduction in the saturated domain, delimited by a free boundary surface moving from the initial position to the steady one. This paper presents a numerical model to analyse the pore pressure regime in slopes stabilized by drain trenches when the soil above the water table is partially saturated. The problem was solved by a 2D free boundary analysis carried out with an original method developed by the authors. It consists of a front-tracking method which is very effective in saving calculation time. Since no explicit solution is available to test the method, the results were compared with those provided by a classical fix-grid method, obtaining differences less than 0.14%. The analysis is carried out inside the saturated domain, where the classical equation of 2D consolidation [2] is used, based on the mechanical principle that the soil porosity changes as a function of effective stresses. On the free boundary, together with the position $U = 0$ (U, pore pressure) the continuity equation is considered, written for an infinitesimal element moving with the free boundary. All along the free boundary the soil compressibility is neglected and the volume at the disposal of the water is represented by a constant value of porosity, equal to the initial one. Water table recharge is considered by means of the term N, which represents the flow entering through the free boundary into the saturated domain. In Section 2 equations valid in the domain and hydraulic boundary conditions are described in dimensional form. In Section 3 an original non-dimensional form of the previous equations and boundary conditions is proposed. In fact the classic form of non-dimensional equation proposed by Terzaghi [2] is not so suitable for the equation adopted on the free boundary. Section 4 deals with the numerical front-tracking method as developed in this work. In Section 5 a dimensional case is solved; the comparison between the proposed method and a classical fix-grid method is presented, stressing the very small differences in results. In Section 6 engineering issues of the problem are investigated, in particular the capability of drain trenches to control the effect of heavy rainfalls. This aspect is treated, calculating limit values of recharge for which water table keeps on constant.

As already emphasized, this work is inserted in a research project related to mathematical modelling of groundwater in slopes stabilized by drain trenches in non-stationary situations. We started by considering the most commonly used consolidation equations. The results obtained agree very well with the experimental data and reveal the capability of predicting the efficiency of drain trenches. Our success prompts us to consider nonlinear models as well, e.g. [3–5]. In this case suitable computational methods of nonlinear problems might be useful, e.g. [6–8].

2. Groundwater in soil between drain trenches

Let us focus our attention on the vertical section between two consecutive trenches, Fig. 1.1. Denote by h the piezometric head

$$h = Z + U/\gamma_w, \tag{2.1}$$

where U is the pore pressure and γ_w the water specific weight. In addition, let

$$F \equiv Z - S(X,T) = 0, \Leftrightarrow Z = S(X,T), \tag{2.2}$$

be the equation of the free surface. When the subsoil is modelled by an isotropic linearly elastic medium, the equation of transient flow in

$$\Omega_T = \{(X,Z) : 0 < X < L, 0 < Z < S(X,T)\} \tag{2.3}$$

is expressed, according to [2], as follows:

$$h_T = c_v \Delta h, \qquad (X,Z) \in \Omega_T, \quad \Delta = \partial_{XX} + \partial_{ZZ}, \tag{2.4}$$

with the consolidation coefficient c_v given by

$$c_v = \frac{KE}{2(1-2\nu)(1+\nu)\gamma_w}, \tag{2.5}$$

where K is the hydraulic conductivity, E the Young modulus and ν the Poisson index.

As illustrated in Fig. 1.1, the depth of the trenches is denoted by H_0 and the height of the analysed domain is indicated by H. With these notations the hydraulic conditions at the boundaries $X = 0$ and $X = L$ are given by

$$\begin{aligned} &\frac{\partial h}{\partial n}(0,Z,T) = 0, \quad 0 < Z < H - H_0, \\ &U(0,Z,T) = 0, \quad H - H_0 \le Z \le S, \end{aligned} \tag{2.6}$$

$$\begin{aligned} &\frac{\partial h}{\partial n}(L,Z,T) = 0, \quad 0 < Z < H - H_0, \\ &U(L,Z,T) = 0, \quad H - H_0 \le Z \le S. \end{aligned} \tag{2.7}$$

The other two boundary conditions are expressed by

$$\frac{\partial h}{\partial n}(X,0,T) = 0, \quad 0 \le X \le L, \tag{2.8}$$

$$U(X,S,T) = 0, \quad 0 < X < L. \tag{2.9}$$

Moreover, because of the continuity requirement, a further equation holds on the free surface, [9],

$$(\mathbf{q} - K\mathbf{N}) \cdot \mathbf{n} = n\mathbf{v} \cdot \mathbf{n}, \tag{2.10}$$

where n denotes the porosity, $\mathbf{v}$ the velocity of propagation of the free surface, $\mathbf{n}$ the outward unit normal and $\mathbf{q}$ the specific discharge at the free surface. In addition, $\mathbf{N}$ denotes the accretion and it is directed vertically downward. In this work it allows for the rain that infiltrates the soil surface and reaches the water table. Negative accretion is due to evaporation or evapotranspiration from the ground surface. N follows a seasonal trend, depending on the rainfall and may be a function of time and space as well. The coefficient K represents the hydraulic conductivity and is introduced for convenience, given that

$$\mathbf{q} = -K\nabla h, \tag{2.11}$$

because of the Darcy law. An alternative form of Eq. (2.10) is the following

$$S_T = -K[1 + U_Z(1 + S_X^2)/\gamma_w - N]/n, \tag{2.12}$$

which appears more suitable for subsequent discussion. Eq. (2.12) was obtained by straightforward calculations which are provided in the Appendix for convenience.

3. Free-boundary problem

By considering relation (2.1), the free-boundary-value problem introduced in Section 2 can be summarized by the following equations:

$$U_T = c_v \Delta U, \qquad (X,Z) \in \Omega_T, \quad T > 0, \tag{3.1}$$

$$\begin{cases} U_X = 0, & X = 0, 0 < Z < H - H_0, T > 0, \\ U = 0, & X = 0, H - H_0 \le Z \le S, T > 0, \end{cases} \tag{3.2}$$

$$U_Z = -\gamma_w, \quad 0 \le X \le L, Z = 0, T > 0, \tag{3.3}$$

$$\begin{cases} U_X = 0, & X = L, 0 < Z < H - H_0, T > 0, \\ U = 0, & X = L, H - H_0 \le Z \le S, T > 0, \end{cases} \tag{3.4}$$

$$U = 0, \quad 0 < X < L, Z = S, T > 0, \tag{3.5}$$

$$S_T = -K[1 + U_Z(1 + S_X^2)/\gamma_w - N]/n, \quad 0 < X < L, Z = S, T > 0. \tag{3.6}$$

Finally, the initial conditions must be prescribed. If it is assumed that the groundwater is initially horizontal at a depth D_w from the ground surface, then

$$S(X, 0) = H - D_w, \quad 0 \le X \le L. \tag{3.7}$$

Furthermore, we also assume

$$U(X, Z, 0) = \gamma_w M(1 - Z/M), \quad 0 \le X \le L, 0 \le Z \le M, \tag{3.8}$$

where

$$M = H - D_w. \tag{3.9}$$

However, we explicitly emphasize that quite general initial conditions can be assigned. Now, the preceding equations are transformed into a non-dimensional form. Use the new unknown functions $u(x, z, t)$ and $s(x, t)$, defined by

$$u = U/U^*, \qquad s = SK/c_v, \tag{3.10}$$

where

$$x = XK/c_v, \qquad z = ZK/c_v, \qquad t = TK^2/c_v, \qquad U^* = \gamma_w c_v/K. \tag{3.11}$$

Hence

$$u_t = \Delta u, \qquad (x, z) \in \Omega_t, \quad t > 0, \tag{3.12}$$

$$\begin{cases} u_x = 0, & x = 0, 0 < z < (H - H_0)K/c_v, t > 0, \\ u = 0, & x = 0, (H - H_0)K/c_v \le z \le s, t > 0, \end{cases} \tag{3.13}$$

$$u_z = -1, \quad 0 \le x \le LK/c_v, z = 0, t > 0, \tag{3.14}$$

$$\begin{cases} u_x = 0, & x = LK/c_v, 0 < z < (H - H_0)K/c_v, t > 0, \\ u = 0, & x = LK/c_v, (H - H_0)K/c_v \le z \le s, t > 0, \end{cases} \tag{3.15}$$

$$u = 0, \quad 0 < x < LK/c_v, z = s, t > 0, \tag{3.16}$$

$$u = MK/c_v - z, \quad 0 \le x \le LK/c_v, 0 \le z \le MK/c_v, t = 0, \tag{3.17}$$

$$s_t = -[1 + u_z(1 + s_x^2) - N]/n, \quad 0 < x < LK/c_v, z = s, t > 0, \tag{3.18}$$

$$s(x, 0) = MK/c_v, \quad 0 \le x \le LK/c_v. \tag{3.19}$$

4. Numerical model

In this section a new front-tracking method is developed for the problem stated in the preceding section. Next, a suitable fixed-grid method will be presented and the results compared.

Let $(x_i, z_{i,k}^j)$ be the generic grid point at time j, where

$$x_i = i\Delta x, \qquad z_{i,k}^j = k\Delta z_i^j, \quad i = 0, \ldots, N_x, k = 0, \ldots, N_z, \tag{4.1}$$

and

$$\Delta x = LK/(c_v N_x), \qquad \Delta z_i^j = s(x_i, t_j)/N_z. \tag{4.2}$$

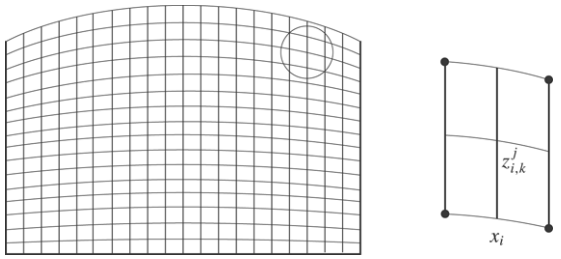

Fig. 4.1. Front-tracking mesh.

Denote by $u^j_i(z^j_{i,k})$ the value of function u at $(x_i, z^j_{i,k}, t_j)$ and, when there is no ambiguous interpretation,

$$u^j_{i,k} = u^j_i(z^j_{i,k}). \tag{4.3}$$

The objective is to find $u^{j+1}_{i,k}$ and s^{j+1}_i when $u^j_{i,k}$ and s^j_i are known. First, note that a solution of (3.12) is approximated by

$$u^{j+1}_i(z^j_{i,k}) = u^j_i(z^j_{i,k}) + r_1\Delta x^2(u_{xx})^j_{i,k} + r^j_{2i}(\Delta z^j_i)^2(u_{zz})^j_{i,k}, \tag{4.4}$$

where

$$r^j_1 = \frac{\Delta t^j}{\Delta x^2}, \qquad r^j_{2i} = \frac{\Delta t^j}{(\Delta z^j_i)^2}. \tag{4.5}$$

The derivative $(u_{xx})^j_{i,k}$ can be functionally related to the mesh points depicted by circles in Fig. 4.1. Indeed, with the positions

$$\delta^{g,h}_{i,k} = z^j_{g,h} - z^j_{i,k}, \tag{4.6}$$

we have

$$\begin{aligned} u^j_{i-1,k+1} &= u^j_{i,k} - (u_x)^j_{i,k}\Delta x + (u_z)^j_{i,k}\delta^{i-1,k+1}_{i,k} + (u_{xx})^j_{i,k}\frac{\Delta x^2}{2} \\ &\quad - (u_{xz})^j_{i,k}\Delta x\delta^{i-1,k+1}_{i,k} + (u_{zz})^j_{i,k}\frac{(\delta^{i-1,k+1}_{i,k})^2}{2}, \end{aligned} \tag{4.7}$$

$$\begin{aligned} u^j_{i-1,k-1} &= u^j_{i,k} - (u_x)^j_{i,k}\Delta x + (u_z)^j_{i,k}\delta^{i-1,k-1}_{i,k} + (u_{xx})^j_{i,k}\frac{\Delta x^2}{2} \\ &\quad - (u_{xz})^j_{i,k}\Delta x\delta^{i-1,k-1}_{i,k} + (u_{zz})^j_{i,k}\frac{(\delta^{i-1,k-1}_{i,k})^2}{2}, \end{aligned} \tag{4.8}$$

$$\begin{aligned} u^j_{i+1,k-1} &= u^j_{i,k} + (u_x)^j_{i,k}\Delta x + (u_z)^j_{i,k}\delta^{i+1,k-1}_{i,k} + (u_{xx})^j_{i,k}\frac{\Delta x^2}{2} \\ &\quad + (u_{xz})^j_{i,k}\Delta x\delta^{i+1,k-1}_{i,k} + (u_{zz})^j_{i,k}\frac{(\delta^{i+1,k-1}_{i,k})^2}{2}, \end{aligned} \tag{4.9}$$

$$\begin{aligned} u^j_{i+1,k+1} &= u^j_{i,k} + (u_x)^j_{i,k}\Delta x + (u_z)^j_{i,k}\delta^{i+1,k+1}_{i,k} + (u_{xx})^j_{i,k}\frac{\Delta x^2}{2} \\ &\quad + (u_{xz})^j_{i,k}\Delta x\delta^{i+1,k+1}_{i,k} + (u_{zz})^j_{i,k}\frac{(\delta^{i+1,k+1}_{i,k})^2}{2}. \end{aligned} \tag{4.10}$$

Summing Eqs. (4.7)–(4.9) and Eqs. (4.8)–(4.10) yields

$$\begin{aligned} u^j_{i-1,k+1} + u^j_{i+1,k-1} &= 2u^j_{i,k} + (u_z)^j_{i,k}(\delta^{i-1,k+1}_{i,k} + \delta^{i+1,k-1}_{i,k}) + (u_{xx})^j_{i,k}\Delta x^2 \\ &\quad + (u_{xz})^j_{i,k}\Delta x\delta^{i+1,k-1}_{i-1,k+1} + \frac{1}{2}\left[(\delta^{i-1,k+1}_{i,k})^2 + (\delta^{i+1,k-1}_{i,k})^2\right](u_{zz})^j_{i,k}, \end{aligned} \tag{4.11}$$

$$u^j_{i-1,k-1} + u^j_{i+1,k+1} = 2u^j_{i,k} + (u_z)^j_{i,k}(\delta^{i-1,k-1}_{i,k} + \delta^{i+1,k+1}_{i,k}) + (u_{xx})^j_{i,k}\Delta x^2 + (u_{xz})^j_{i,k}\Delta x\delta^{i+1,k+1}_{i-1,k-1} + \frac{1}{2}\left[(\delta^{i-1,k-1}_{i,k})^2 + (\delta^{i+1,k+1}_{i,k})^2\right](u_{zz})^j_{i,k}. \tag{4.12}$$

From the last two equations it follows that:

$$(u_{xx})^j_{i,k} = \frac{1}{\gamma_{i,k}\Delta x^2}\left[(u^j_{i-1,k+1} + u^j_{i+1,k-1})\delta^{i+1,k+1}_{i-1,k-1} - 2\gamma_{i,k}u^j_{i,k} - \rho_{i,k}(u_{zz})^j_{i,k}/2 - \nu_{i,k}(u_z)^j_{i,k} - (u^j_{i-1,k-1} + u^j_{i+1,k+1})\delta^{i+1,k-1}_{i-1,k+1}\right], \tag{4.13}$$

where

$$\gamma_{i,k} = \delta^{i+1,k+1}_{i-1,k-1} - \delta^{i+1,k-1}_{i-1,k+1}, \tag{4.14}$$

$$\nu_{i,k} = (\delta^{i-1,k+1}_{i,k} + \delta^{i+1,k-1}_{i,k})\delta^{i+1,k+1}_{i-1,k-1} - (\delta^{i-1,k-1}_{i,k} + \delta^{i+1,k+1}_{i,k})\delta^{i+1,k-1}_{i-1,k+1}, \tag{4.15}$$

$$\rho_{i,k} = \left[(\delta^{i-1,k+1}_{i,k})^2 + (\delta^{i+1,k-1}_{i,k})^2\right]\delta^{i+1,k+1}_{i-1,k-1} - \left[(\delta^{i-1,k-1}_{i,k})^2 + (\delta^{i+1,k+1}_{i,k})^2\right]\delta^{i+1,k-1}_{i-1,k+1}. \tag{4.16}$$

Substituting $(u_z)^j_{i,k}$ in (4.13) by the central approximation provides the desired expression for $(u_{xx})^j_{i,k}$:

$$(u_{xx})^j_{i,k} = \frac{1}{\gamma_{i,k}\Delta x^2}\left[(u^j_{i-1,k+1} + u^j_{i+1,k-1})\delta^{i+1,k+1}_{i-1,k-1} - 2\gamma_{i,k}u^j_{i,k} - \rho_{i,k}(u_{zz})^j_{i,k}/2 - \nu_{i,k}(u^j_{i,k+1} - u^j_{i,k-1})/2\Delta z^j_i - (u^j_{i-1,k-1} + u^j_{i+1,k+1})\delta^{i+1,k-1}_{i-1,k+1}\right]. \tag{4.17}$$

Now, inserting this result into Eq. (4.4) yields

$$\begin{aligned} u^{j+1}_i(\zeta^j_{i,k}) = {} & \left[1 - 2r^j_1 - 2r^j_{2i} + \frac{(\hat{r}_1)^j_{i,k}\rho_{i,k}}{(\Delta z^j_i)^2}\right]u^j_{i,k} \\ & + (\hat{r}_1)^j_{i,k}\delta^{i-1,k+1}_{i+1,k-1}\left[u^j_{i-1,k-1} + u^j_{i+1,k+1}\right] + (\hat{r}_1)^j_{i,k}\delta^{i+1,k+1}_{i-1,k-1}\left[u^j_{i-1,k+1} + u^j_{i+1,k-1}\right] \\ & + \left[r^j_{2i} - \frac{(\hat{r}_1)^j_{i,k}\rho_{i,k}}{2(\Delta z^j_i)^2} + \frac{(\hat{r}_1)^j_{i,k}\nu_{i,k}}{2\Delta z^j_i}\right]u^j_{i,k-1} + \left[r^j_{2i} - \frac{(\hat{r}_1)^j_{i,k}\rho_{i,k}}{2(\Delta z^j_i)^2} - \frac{(\hat{r}_1)^j_{i,k}\nu_{i,k}}{2\Delta z^j_i}\right]u^j_{i,k+1}, \end{aligned} \tag{4.18}$$

where the central approximation has been used for $(u_{zz})^j_{i,k}$ and, in addition,

$$(\hat{r}_1)^j_{i,k} = r^j_1/\gamma_{i,k}.$$

Straightforward calculations show that method (4.18) is stable if

$$1 - 2r^j_1 - 2r^j_{2i} + \frac{(\hat{r}_1)^j_{i,k}\rho_{i,k}}{(\Delta z^j_i)^2} \geq 0, \tag{4.19}$$

$$r^j_{2i} - \frac{(\hat{r}_1)^j_{i,k}\rho_{i,k}}{2(\Delta z^j_i)^2} \pm \frac{(\hat{r}_1)^j_{i,k}\nu_{i,k}}{2\Delta z^j_i} \geq 0. \tag{4.20}$$

Remark 4.1. For rectangular mesh characterized by

$$r_1 = \Delta t/\Delta x^2, \qquad r_2 = \Delta t/\Delta z^2, \tag{4.21}$$

it is $\gamma_{i,k} = 4\Delta z$, $\rho_{i,k} = 8\Delta z^3$, $\nu_{i,k} = 0$, and the conditions (4.19) and (4.20) reduce to

$$1 - 2r_2 \geq 0, \quad r_2 - r_1 \geq 0. \tag{4.22}$$

Table 5.1
S_1 (fix-grid method) and S_2 (front-tracking method)

X	0	1.0	2.0	3.0	4.0	5.0	6.0	7.0	8.0	9.0	10.0
S_1	9.387	9.478	9.570	9.643	9.670	9.742	9.774	9.796	9.811	9.820	9.823
S_2	9.391	9.479	9.567	9.638	9.692	9.733	9.763	9.784	9.798	9.806	9.809

Furthermore, Eq. (4.18) becomes

$$u_{i,k}^{j+1} = (1-2r_2)u_{i,k}^{j} + (r_2-r_1)(u_{i,k-1}^{j} + u_{i,k+1}^{j}) + r_1(u_{i-1,k-1}^{j} + u_{i+1,k+1}^{j} + u_{i-1,k+1}^{j} + u_{i+1,k-1}^{j})/2. \tag{4.23}$$

Note that (4.23) does not reduce to the classical explicit method, e.g. [10]. This also emphasizes the novelty of algorithm (4.18).

Eq. (4.18) provides $u_i^{j+1}(z_{i,k}^{j})$. To obtain $u_i^{j+1}(z_{i,k}^{j+1})$ consider

$$u_i^{j+1}(z_{i,k}^{j}) = u_i^{j+1}(z_{i,k}^{j+1}) + (u_z)_{i,k}^{j+1}(z_{i,k}^{j+1})[z_{i,k}^{j} - z_{i,k}^{j+1}] + (u_{zz})_{i,k}^{j+1}(z_{i,k}^{j+1})[z_{i,k}^{j} - z_{i,k}^{j+1}]^2/2. \tag{4.24}$$

Hence, by using the central approximations for both partial derivatives and the position

$$d_i^{j} = [z_{i,k}^{j} - z_{i,k}^{j+1}]/\Delta z_i^{j+1}, \tag{4.25}$$

it follows that:

$$u_i^{j+1}(z_{i,k-1}^{j+1})[(d_i^{j})^2 - d_i^{j}]/2 + u_i^{j+1}(z_{i,k}^{j+1})[1-(d_i^{j})^2] + u_i^{j+1}(z_{i,k+1}^{j+1})[(d_i^{j})^2 + d_i^{j}]/2 = u_i^{j+1}(z_{i,k}^{j}). \tag{4.26}$$

Solving this system gives the pressure $u_i^{j}(z_{i,k}^{j+1})$. Finally, the free boundary is obtained by

$$s_i^{j+1} = s_i^{j} - \Delta t^{j}\{1 + u_z(x_i, s_i^{j}, t_j)[1 + s_x^2(x_i, t_j)] - N_i^{j}\}/n, \tag{4.27}$$

with

$$u_z(x_i, s_i^{j}, t_j) = (3u_{i,N_z}^{j} - 4u_{i,N_z-1}^{j} + u_{i,N_z-2}^{j})/2\Delta z_i^{j}, \tag{4.28}$$

$$s_x(x_i, t_j) = (s_{i+1}^{j} - s_{i-1}^{j})/2\Delta x. \tag{4.29}$$

5. Discussion of preliminary results

First, the new computational method is tested by using the following special data:

$$c_v = 3.8 \times 10^{-6}\ \mathrm{m^2/s}, \qquad K = 10^{-8}\ \mathrm{m/s}, \tag{5.1}$$

$$L = 20\ \mathrm{m}, \qquad H = 10\ \mathrm{m}, \qquad H_0 = 5\ \mathrm{m}, \qquad D_w = N = 0. \tag{5.2}$$

Since, to our knowledge, no explicit solution is available for the free-boundary-value problem (3.12)–(3.19), the numerical results provided by the front-tracking method are compared with those obtained by a suitable fix-grid method. Here, the evolution of the free surface is obtained by Eq. (3.18) and the solution of Eq. (3.12) is computed by the classical explicit method, e.g. [10],

$$u_{i,k}^{j+1} = (1-2r_1-2r_2)u_{i,k}^{j} + r_1(u_{i-1,k}^{j} + u_{i+1,k}^{j}) + r_2(u_{i,k-1}^{j} + u_{i,k+1}^{j}). \tag{5.3}$$

For $T = 365$ days, the free boundaries are depicted in Fig. 5.1 and the numerical values are compared in Table 5.1. Since S is symmetrical, only the results for $0 \le X \le 10$ are reported. Note a difference no greater than 0.14%.

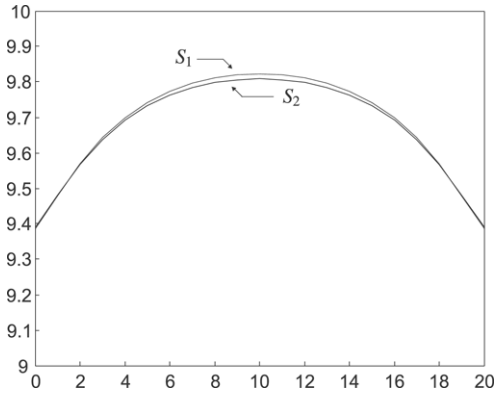

Fig. 5.1. S_1 (fix-grid method) and S_2 (front-tracking method).

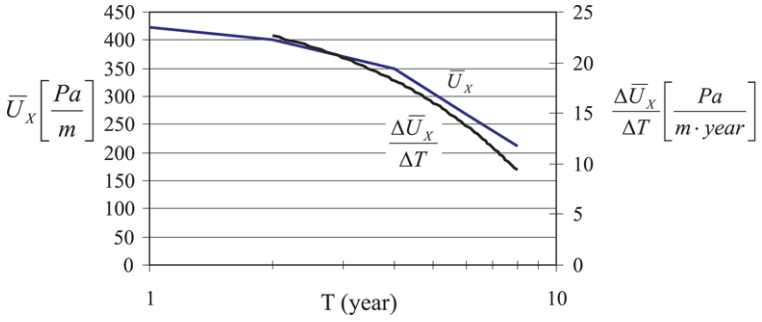

Fig. 6.1. $\bar{U}_X$ (it is the average of the function U_x along the segment $H - Ho \leq Z \leq S$) and $\Delta\bar{U}_X/\Delta T$ against time, from the initial condition.

6. Results of analysis

The transient process from the initial condition to the steady one was analysed for a case in which the consolidation process is very slow. Geometrical and soil parameters are those indicated in Section 5: thus at the initial condition ($T = 0$) the water table is at the ground surface, from which there is no recharge to the water table ($N = 0$). During the transient phenomenon, from $T = 0$ to the steady condition ($T = \infty$), water flow toward the trenches decreases with time: this is shown in Fig. 6.1 where the average value $\bar{U}_X$, calculated along the segment $H - Ho \leq Z \leq S$ is reported against time. The velocity of the process calculated as $\Delta\bar{U}_X/\Delta T$ decreases quickly with time: this means that nevertheless the phenomenon is longlasting the water table is markedly lowered in the first period of the trench work. This is an important result for engineering applications.

Results presented in Figs. 6.2–6.4 are the solution of the problem for different times: at the initial condition, one year after, eight years after the beginning of trench work. In each figure two axes are reported: on the left there is the height above the $Z = 0$ plane, useful to locate the free boundary position, on the right there is the scale of pore pressure, useful to represent the envelope of pore pressure on the plane through the base of the trenches. The position of the free boundary allows us to determine the height of the trench which is working at the time considered (it is the height below the free surface). The envelope of pore pressure on a deep plane allows the efficiency of the trench to be assessed on that plane. In this case for simplicity the plane for the base of the trenches is chosen, but when the position of the slip surface is known, pore pressures have to be determined along it. It can be seen that the free boundary (whose position is essential to fix the boundary condition on the trench wall) is well above the pore pressure envelope. This means that a large part of the height of the trench works even after a long time from the beginning of drainage and trenches are always ready to discharge water flow of heavy rains. This justifies the capability of drain trenches of avoiding pore pressure peaks during wet seasons. Indeed, previous analyses and measurements carried out on instrumented sites [1] where drain trenches were constructed, show that the water table is not subject to seasonal fluctuations as it occurs in the absence of drains. This behaviour can be modelled imposing $S_T = 0$ in Eq. (2.12) or $s_t = 0$ in Eq. (3.18). This was done after one year of water table lowering characterized by $N = 0.2$ (which can

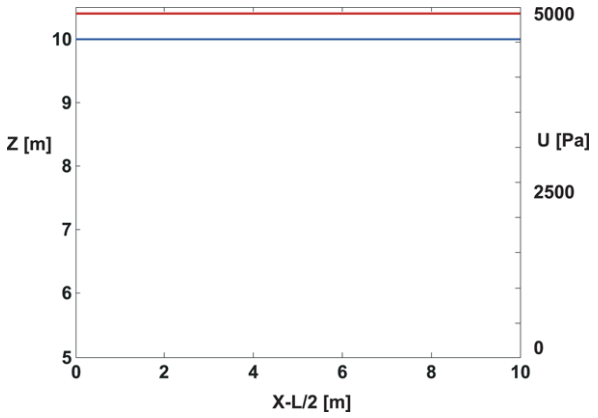

Fig. 6.2. Initial condition: The free boundary surface (above), represented respect to the axis of height (on the left, in m) and the envelope of pore pressure (below) on the plane through the base of the trenches, represented respect to the axis of pressure (on the right, in Pa).

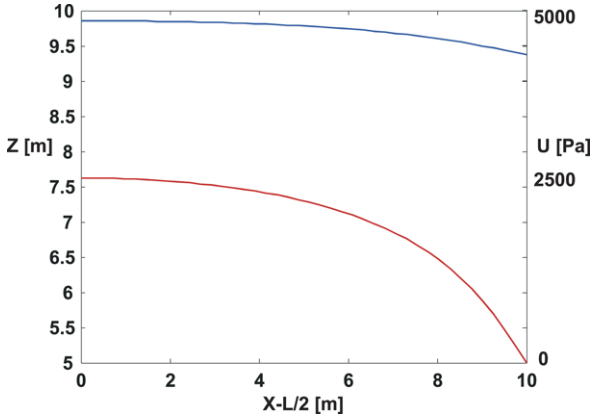

Fig. 6.3. The free boundary surface (above) and the envelope of pore pressure (below) on the plane through the base of the trenches, after one year from the beginning of the trench work.

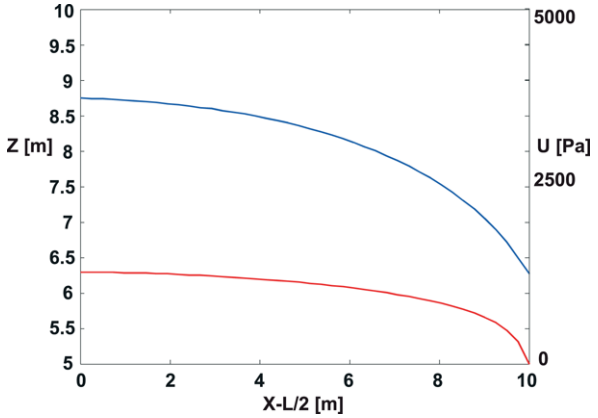

Fig. 6.4. The free boundary surface (above) and the envelope of pore pressure (below) on the plane through the base of the trenches, after eight years from the beginning of the trench work.

be considered a likely yearly average of water table recharge). A heavy rainfall is thus simulated, to investigate the response of the trenches (rainfall is simply schematized by accretion N). Values of accretion are calculated, for which the water table remains constant; the duration of the event is also considered (Fig. 6.5). These values define a curve

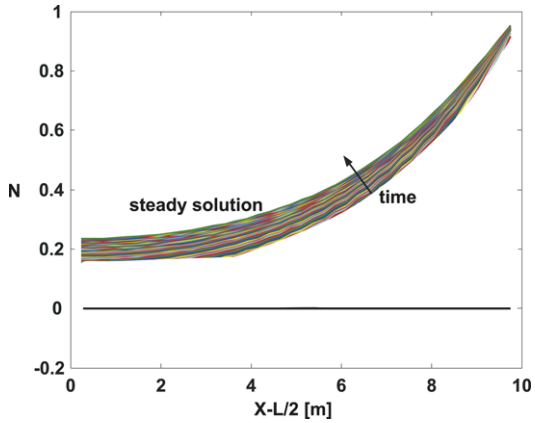

Fig. 6.5. Values of accretion N for which S keeps on constant, against the distance of the considered point from the middle axis of the trenches.

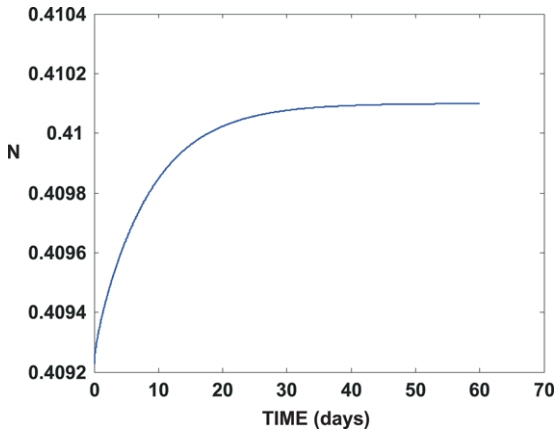

Fig. 6.6. Values of accretion N_∞ for which $\bar{S}_\infty$ keeps on constant, against the duration of the rainfall.

above which there are critical rainfalls that can induce an increase in pore pressure in the subsoil. Due to recharge, the profile of the water table between the trenches greatly changes. This is shown by Fig. 6.5 that shows N values for which the water table remains at the same level, against the distance of the considered point from the middle axis of the trenches. Over time, from the beginning of rainfall, N increases up to the steady value: with the duration of the rainfall, the ability of drain trenches to discharge water infiltrating in the subsoil also increases. In the middle, low values of N ($\geq$0.2) can lead the water table to rise; near trenches also the larger values of N ($\approx$1) are unable to increase pore pressure in the subsoil. Given the value $\bar{S}_\infty$ that expresses the average of the function $S(X, T)$ for $0 < X < L$ at $T = \infty$, it can be seen in Fig. 6.6 that trenches (arranged at a relative distance of 20 m) are able to discharge water infiltrating in the subsoil, without increasing pore pressure in the slope, up to $N = 0.41$.

The value $N = 0.41$ is large enough for engineering applications, given that the maximum infiltration in the subsoil (after a small initial period from the beginning of rainfall) is 1, [11], and that part of the infiltration goes back to the atmosphere in evaporation and evapotranspiration. As a consequence a design with a small distance between trenches improves the ability of the drain system to prevent the critical effects of heavy rainfalls.

7. Conclusion

The important role of drains working in unstable slopes is shown through an analysis with a new computational method developed in this work. A case typical of medium grained soil was considered, in which the soil above the water table is partially saturated. Therefore a boundary surface can be recognized between the saturated domain (water table) and the unsaturated one (above the water table); the problem is solved by calculating the motion of the free boundary. The new computational method consists of a front-tracking method which is very effective in saving

calculation time compared with fix-grid methods. It has been shown that also for rectangular mesh the new method does not reduce to the classical explicit method. Because no explicit solution is available for the free-boundary problem the numerical results, provided by the front-tracking method, were compared with those obtained by a suitable fix-grid method. Differences are less than 0.14%.

The results were used to investigate the efficiency of the trenches in transient conditions. During the phase of water table lowering, characterized by no water recharge, a heavy rainfall was simulated to describe the response of the trenches. Values of accretion were calculated, for which the water table remains constant, as a function of the duration of the event. The results define a curve, above which rainfalls are critical and induce an increase in pore pressure in the slope. It was shown that up to large values of recharge, trenches are able to discharge water infiltrating in the subsoil, without increasing the pore pressure. This capability is a function of the relative distance between trenches that is the most important design element to improve the capability of the drain system in preventing the critical effects of heavy rainfalls.

Appendix

In this appendix we briefly provide the calculations which lead to Eq. (2.12). From (2.10) and (2.11) it follows that:

$$-K(\nabla h + \mathbf{N}) \cdot \mathbf{n} = n\mathbf{v} \cdot \mathbf{n}, \tag{A.1}$$

where

$$\mathbf{n} = \nabla F/|\nabla F|, \quad \nabla F = (-S_X, 1), \tag{A.2}$$

and

$$\mathbf{N} = -N\mathbf{k}, \quad \mathbf{k} = \text{unit vector directed as } z. \tag{A.3}$$

In addition, Eq. (2.2) implies

$$F_T + \nabla F \cdot \mathbf{v} = 0, \tag{A.4}$$

with $F_T = -S_T$. Insert the last results into Eq. (A.1) to get

$$-K(\nabla h \cdot \nabla F - N) = nS_T. \tag{A.5}$$

Since h is related to U by the relation (2.1), it is

$$\nabla h = (U_X/\gamma_w, 1 + U_Z/\gamma_w). \tag{A.6}$$

On the other hand, from $U(X, S(X, T)) = 0$ it follows that:

$$U_X = -S_X U_Z. \tag{A.7}$$

Insert (A.6) and (A.7) into Eq. (A.5) to obtain

$$nS_T = -K[1 + U_Z(1 + S_X^2)/\gamma_w - N], \tag{A.8}$$

which is exactly Eq. (2.12).

References

[1] B. D'Acunto, G. Urciuoli, Groundwater regime in a slopes stabilized by drain trenches, Math. Comput. Modelling 43 (2006) 745–765.
[2] T.W. Lambe, R.V. Whitman, Soil Mechanics, J. Wiley & Sons Inc., New York, 1969.
[3] R. De Boer, Highlights in the historical development of the pourous media: Toward a consistent macroscopic theory, Appl. Mech. Rev. 49 (1996) 201–262.
[4] R. De Boer, Theory of Porous Media. Highlights in Historical Development and Current State, Springer-Verlag, Berlin, 2000.
[5] M. Battaglio, N. Bellomo, I. Bonzani, R. Lancellotta, Non-linear consolidation models of clay which change type, Internat. J. Non-linear Mech. 38 (2003) 493–500.
[6] N. Bellomo, E. De Angelis, L. Graziano, A. Romano, Solution of nonlinear problems in applied sciences by generalized collocation methods and Matematica, Comput. Math. Appl. 41 (2001) 1343–1363.

[7] J. Rappaz, A. Reist, Mathematical and numerical analysis of a three dimensional fluid flow model in glaciology, Math. Models Methods Appl. Sci. 15 (2005) 37–52.
[8] F. Brezzi, K. Lipnikov, V. Simoncini, A family of mimetic finite difference methods on polygonal and polyhedral meshes, Math. Models Methods Appl. Sci. 15 (2005) 1533–1551.
[9] J. Bear, Dynamics of Fluids in Porous Media, Elsevier Publishing Company, New York, 1972.
[10] B. D'Acunto, Computational Methods for PDE in Mechanics, World Scientific, Singapore, 2004.
[11] G.E. Blight, Interaction between the atmosphere and the Earth, Geotechnique 47 (1997) 715–766.